Received: 14 October 2021 | Revised: 3 May 2022 | Accepted: 21 May 2022

DOI: 10.1111/gcb.16317

Global Change Biology WILEY

RESEARCH ARTICLE

# Biological sensitivities to high-resolution climate change projections in the California current marine ecosystem

Jennifer M. Sunday[1] | Evan Howard[5] | Samantha Siedlecki[3] | Darren J. Pilcher[4] | Curtis Deutsch[5,6] | Parker MacCready[2] | Jan Newton[7] | Terrie Klinger[8]

[1]Department of Biology, McGill University, Montreal, Quebec, Canada

[2]School of Oceanography, University of Washington, Seattle, Washington, USA

[3]Department of Marine Sciences, University of Connecticut, Groton, Connecticut, USA

[4]Cooperative Institute for Climate, Ocean, and Ecosystem Studies, University of Washington, Seattle, Washington, USA

[5]Department of Geosciences, Princeton University, Princeton, New Jersey, USA

[6]High Meadows Environmental Institute, Princeton University, Princeton, New Jersey, USA

[7]Applied Physics Laboratory, University of Washington, Seattle, Washington, USA

[8]School of Marine and Environmental Affairs, University of Washington, Seattle, Washington, USA

**Correspondence**
Jennifer M. Sunday, Department of Biology, McGill University, Montreal, Quebec H3A 1B1, Canada.
Email: jennifer.sunday@mcgill.ca

**Funding information**
Schwab Charitable Fund

## Abstract

The California Current Marine Ecosystem is a highly productive system that exhibits strong natural variability and vulnerability to anthropogenic climate trends. Relating projections of ocean change to biological sensitivities requires detailed synthesis of experimental results. Here, we combine measured biological sensitivities with high-resolution climate projections of key variables (temperature, oxygen, and $pCO_2$) to identify the direction, magnitude, and spatial distribution of organism-scale vulnerabilities to multiple axes of projected ocean change. Among 12 selected species of cultural and economic importance, we find that all are sensitive to projected changes in ocean conditions through responses that affect individual performance or population processes. Response indices were largest in the northern region and inner shelf. While performance traits generally increased with projected changes, fitness traits generally decreased, indicating that concurrent stresses can lead to fitness loss. For two species, combining sensitivities to temperature and oxygen changes through the Metabolic Index shows how aerobic habitat availability could be compressed under future conditions. Our results suggest substantial and specific ecological susceptibility in the next 80 years, including potential regional loss of canopy-forming kelp, changes in nearshore food webs caused by declining rates of survival among red urchins, Dungeness crab, and razor clams, and loss of aerobic habitat for anchovy and pink shrimp. We also highlight fillable gaps in knowledge, including specific physiological responses to stressors, variation in responses across life stages, and responses to multistressor combinations. These findings strengthen the case for filling information gaps with experiments focused on fitness-related responses and those that can be used to parameterize integrative physiological models, and suggest that the CCME is susceptible to substantial changes to ecosystem structure and function within this century.

KEYWORDS
California current marine ecosystem, carbon dioxide, climate change, oxygen, physiological sensitivity, regional climate projections, species vulnerability, temperature

## 1 | INTRODUCTION

Anthropogenic climate change and associated stressors will cause profound changes in global ocean conditions, in species distributions, and in the services the ocean provides to society (Gattuso et al., 2015; Pecl et al., 2017). Global models predict that changes in ocean pH, temperature, and oxygen concentration will force changes in critical earth system processes such as biogeochemical cycling and in marine ecosystem structure and function. These changes will ultimately affect human well-being and food security (Henson et al., 2017; Pecl et al., 2017; Pörtner et al., 2014). Recent work has estimated the vulnerability of species and functional groups to climate-associated changes in the ocean through consensus of the international climate community combined with physical or biological data (Gattuso et al., 2015; Hare et al., 2016; Hollowed et al., 2020; Spencer et al., 2019). Such analyses offer means of anticipating biological and ecological changes and can be used to help promote human adaptation to impending changes; they are likely to be most useful when supported by quantitative data on biological responses to environmental change.

Here, we combine a data-driven analysis of biological sensitivities to environmental change with high-resolution dynamically downscaled regional climate projections to describe biological vulnerabilities to climate change in the California Current Marine Ecosystem (CCME). The CCME comprises an upwelling-dominated eastern boundary current system with known vulnerabilities to climate-associated stressors including warming, oxygen loss, and ocean acidification variables (Chan et al., 2008; Connolly et al., 2010; Feely et al., 2008; McCabe et al., 2016). We use regionally downscaled climate projections of multiple variables (temperature, oxygen, and carbon dioxide [$CO_2$]) that combine the effects of changing surface winds, heat fluxes, atmospheric $CO_2$, terrestrial freshwater inputs, and physical and biogeochemical cycling to generate end-of-century projections of ocean conditions at high resolutions that can resolve some coastal processes (Howard, Frenzel, et al., 2020; Siedlecki et al., 2021). We evaluate four key variables—temperature, salinity, oxygen, and $pCO_2$ or its covariate, pH—that are influenced by anthropogenic carbon emissions, in terms of their expected influences on organismal physiology. These include the observed experimental effects of these stressors on growth, metabolic rate, reproduction, survivorship, and behavior. Although we aggregate and report sensitivies across life-history stages, we exclude consideration of how these interact with seasonal changes due to problems of data sufficiency. Here, we present an approach to first evaluate the biological sensitivities of key species to projected climate-associated changes in the CCME, and next to map the spatially variable climate vulnerability of these species. As such, our analysis offers a generalizable approach to assessing and comparing conservative estimates of potential risk and habitat vulnerability across taxa exposed to climate stressors.

Our approach differs from prior studies that, by necessity, used expert judgment concerning biological responses (e.g., Bednaršek et al., 2019; Gattuso et al., 2015), used downscaled projections of single stressors (e.g., Hodgson et al., 2018; Marshall et al., 2017; Morley et al., 2018), or combined response data across broad taxonomic groups to assess vulnerability to projected changes in ocean conditions (e.g., Busch & McElhany, 2016). Here, we use experimental evidence of direct effects on physiological performance of 10 key species or closely related species groups, and use inferred sensitivities based on a well-understood mechanistic model of the physiological response to multiple stressors for two others. Each of the species considered provides direct or indirect benefits to ecosystem function, cultural and economic services, and human well-being. We find a range of sensitivities across these species and explore the interactions between physiological responses and spatial variation in projected climate exposure. In particular, we identify regions of the CCME in which many of the species evaluated are vulnerable to climate change, including species that have multiple physiological vulnerabilities.

## 2 | METHODS

### 2.1 | Regional climate projection models and future forcing

We projected ocean conditions by downscaling global Earth system models at coarse spatial resolution (~100 km) to two finer resolutions (12 and 1.5 km models) as described in Siedlecki et al. (2021). Both regional modeling frameworks employ the Regional Ocean Modeling System (ROMS). The higher resolution (1.5 km) simulation of the northern CCME was optimized for the Pacific Northwest "Cascadia" region spanning most of Oregon, Washington, and some of Vancouver Island (43°N to 50°N), and includes freshwater forcing from major rivers such as the Columbia and Fraser Rivers. The 12 km model is configured for a domain that extends along the North American west coast from 25°N to 60°N, described in more detail in Howard, Frenzel, et al. (2020).

One hundred-year climate change forcings for the CCME 12 km simulation were based on the differences between climatological monthly conditions in 1971–2000 and 2071–2100 conditions, projected using representative concentration pathway 8.5 (RCP 8.5, the "business as usual" scenario) for five models from the CMIP5 archive: GFDL (ESM2M), IPSL (CM5A-LR), Hadley (ES), MPI (ESM-LR), and NCAR (CESM) (see Howard, Frenzel, et al. (2020) for the rationale for model choice). Downscaled climate projections were produced by resimulating the CCME over the hindcast years 1994–2007 with the addition of these hundred-year differences to the historical forcings. Climate forcings included net downward radiation, wind speed, air temperature, and specific humidity, as well as initial conditions and boundary anomalies in biogeographic variables (dissolved oxygen, nitrate, phosphate, silica, iron, inorganic carbon, and alkalinity). The 1.5 km resolution model is one-way nested within the 12 km resolution model and is run for 3-year "time slices" covering 2002–2004 for the control simulation and 2094–2096 for the future projection simulation. In both simulations, we ran the model for 1 year

(i.e., model spin-up) before we used the output for our analysis, using 2001 forcing for the control and 2093 forcing for the future projection. The much shorter time slice for the 1.5 km resolution model reflects the substantially greater computational costs. Full details of the 1.5 km simulation can be found in Siedlecki et al. (2021).

Carbonate system variables (i.e., pH, $pCO_2$, and carbonate saturation state [Ω] values) were computed with CO2SYS (Lewis & Wallace, 1998) using model output fields of dissolved inorganic carbon (DIC), total alkalinity (TA), temperature, and salinity. We generated annual averages of variables in each model cell prior to calculating a spatially weighted mean, and calculated differences in temperature, oxygen, pH, and $pCO_2$ between the two time periods (i.e., deltas) for every grid cell. For downstream analysis, we extracted conditions for three ocean layers: (1) surface conditions, drawn from the uppermost model layer for each simulation; (2) bottom conditions, drawn from the deepest vertical layer; and (3) depth-averaged ocean conditions, calculated as the mean between the surface and 200 m depth (or to the bottom depth in shallower waters).

## 2.2 | Physiological sensitivities

We selected for analysis 12 taxa representing individual species or closely related and functionally similar species groups (hereafter referred to simply as "species") known to be of high cultural and ecological significance in the CCME (Table 1). To evaluate the future effects of ocean change on these species, we used two distinct but complementary approaches. First, for 10 species, we compiled experimental results from the published literature that measured organism-level responses to one or more of four ocean variables expected to shift in the CCME in association with climate change. Second, for two species, we used the Metabolic Index of temperature-dependent hypoxia response (Φ; Deutsch et al., 2015) to assess potential organism-level response to the combined multiple-stressor impacts of temperature and oxygen, variables with robust climate trends across CCME models (Howard, Frenzel, et al., 2020; Siedlecki et al., 2021).

## 2.3 | Experimental sensitivities to individual stressors

We used published data from controlled experiments to estimate sensitivities. We searched the published literature for controlled experiments in which (i) temperature, oxygen, $pCO_2$, and/or salinity were varied within the range of mean values expected between the present and year 2100 in the California Current Marine Ecosystem and (ii) the individual-level response of these species was measured in one or more of the following categories: survival, metabolic rate, locomotion, somatic growth rate, and resource consumption rate. Note that responses to experimental variation in pH or $pCO_2$ were used as estimates of sensitivity to changing carbonate chemistry, which, for the purposes of this analysis, we considered as a single stressor. In three cases (canopy-forming kelps, blue and black rockfish, and copper and quillback rockfish), we aggregated data from more than one species in order to increase data coverage within those groups (Table S1). We extracted either (i) all individual-level observations of the response variable (including control treatments) or (ii) the mean, error estimate, and sample size of aggregated response data. When values were not reported as numbers, we estimated

**TABLE 1** Species and groups of species included in analyses, with common and Latin names, depth ranges occupied, and layers of the model domain used for adults and early life stages for which we had data. Information sources are provided in the supplemental dataset.

| Common name | Species included | Lower depth (m) | Upper depth (m) | Adult zone | Early-life-stage zone |
|---|---|---|---|---|---|
| Direct single-stressor responses | | | | | |
| Pink salmon | *Oncorhynchus gorbuscha* | 250 | 0 | 200 m | NA |
| Blue rockfish and Black rockfish | *Sebastes mystinus*, *Sebastes melanops* | 550 | 0 | Bottom | NA |
| Copper rockfish and Quillback rockfish | *Sebastes caurinus*, *Sebastes maliger* | 366 | 0 | Bottom | NA |
| Sablefish | *Anoplopoma fimbria* | 2740 | 175 | Bottom | NA |
| Razor clam | *Siliqua patula* | 55 | 0 | Bottom | NA |
| Red urchin | *Mesocentrotus franciscanus* | 125 | 0 | Bottom | Surface/bottom[a] |
| Dungeness crab | *Metacarcinus magister* | 360 | 0 | Bottom | Surface |
| Ochre star | *Pisaster ochraceus* | 90 | 0 | Bottom | Surface |
| Canopy-forming kelp | *Macrocystis pyrifera*, *Nereocystis luetkeana* | 30 | 0 | Bottom | Bottom |
| Seagrass | *Zostera marina* | 10 | 0 | Bottom | NA |
| Range projection using Metabolic Index | | | | | |
| Northern anchovy | *Engraulis mordax* | | | | |
| Alaska pink shrimp | *Pandalus eous* | | | | |

[a]Gametes of red urchins were restricted to the deep layer of the model; larvae were restricted to the surface layer.

values from figures using WebPlotDigitizer (Rohatgi, 2018). In addition to the category of response, we noted the location of organism collection, experimental treatments, duration of exposure, life phase, and other environmental variables for each experiment. We included published studies through December of 2020.

Because the response values and associated units varied across experiments, we transformed these data to allow comparison of effect sizes. We did this by (i) inverting mortality rates so that they aligned with survival rates, (ii) converting uncertainty estimates to standard errors of the mean (using SE = 95% confidence interval/1.96), (iii) recentering data so that physiologically unreasonable negative values (1% of data) did not go below zero, (iv) standardizing values to a reference value, by dividing each observation by the highest observed value (reference) within each experiment (or, for aggregated data, to the highest observed aggregate value plus 1 standard error). The resulting effect sizes ranged between 0 and 1.

To map connect the sensitivity of each taxon to each environmental variable, we developed a simple sensitivity index based on these comparable effect sizes. First, we filtered out data in which treatment values were outside the range of present and future projections of each variable (temperature: 8.7–30.8°C, oxygen: 0.003–6.73 mL/L, $pCO_2$: 298–3090 µatm, salinity: 29.0–33.5 ppt). For studies in which only means and standard errors were available, we simulated sampling error by iteratively drawing *N* values at each treatment level, where *N* is the experimental sample size of each treatment, from a normal distribution with the reported mean and error for each treatment level. We fit a linear regression (Model I) to each random draw, and calculated the mean and standard error of the slope and intercept across 5000 iterations. For non-aggregated data, we fit linear regressions (Model I) to the individual observations of each experiment. We refer to this population of comparably fitted slopes in response variables with associated uncertainty estimates as the estimated *sensitivities* of organisms to individual components of environmental change.

Within the relevant ranges of each environmental variable, almost all responses were monotonic; individual linear regressions through these responses had relatively good fits and allowed us to consider a single variable (slope) as the metric of relative sensitivity (Figure S1–S4). However, a small number of nonlinearities in temperature and oxygen responses within the present-to-future environmental domain in sablefish and Dungeness crab suggest some fitted slopes will represent underestimates of sensitivity (see Figures S2–S3).

## 2.4 | Data aggregation and scaling

We aggregated and scaled taxon sensitivities in various ways for display. First, in order to visually compare all sensitivities across exposure types that vary in magnitude, we multiplied each sensitivity by the mean projected change in environmental variable (delta) projected between the present (1971–2000) and future (2071–2100) periods for the subset of grid cells in the model domains within the focal taxon's known depth distribution. For each sensitivity estimate, we used environmental deltas projected for the depth stratum (surface, bottom, or upper 200 m mean) relevant for the life-history stage studied: bottom for benthic and demersal stages (most species and life stages in the dataset), the upper 200 m depth range for epipelagic organisms (pink salmon), and surface values for larvae found in the surface mixed layer (e.g., sea urchin larvae, Table 1). We refer to these products, that is, the individual experimentally derived sensitivities multiplied by the downscaled climate projections, as *scaled sensitivities* (although we note that these could also be considered as estimated responses given that they are the product of sensitivity and exposure).

## 2.5 | Response indices across space

In order to summarize these scaled sensitivities for each taxon and response type, while synthesizing across environmental variables, we used a meta-analysis approach, taking a weighted mean of scaled sensitivities within taxon and response types. Weights were assigned as the inverse of the squared variance of each sensitivity, and overall variance as the inverse of the summed weights (Lipsey & Wilson, 2001). We thus combined responses to different aspects of environmental change (temperature, $O_2$, pH or $pCO_2$) *within* response types (metabolic rate, growth rate, consumption rate, motility rate, and survival rate) allowing responses to be additive within but not across response types. For example, we additively combined increases with decreases in growth rates for a red urchin, even if these responses were driven by temperature and $pCO_2$, respectively. Although different stressors are known to have interactive effects on physiological responses (Crain et al., 2008), this additive approach provides a first-cut level of data aggregation in the absence of interaction data or mechanistic models, and when possible we apply a mechanistic model of interactive effects between stressors in our Metabolic Index approach (below). We report these meta-analyzed results at two aggregated scales, first based on mean scaled sensitivies in biological rates for each taxon and response type across the entire model domain (still within relavent grid cells for each species) to assess taxon level differences, and second, based on mean projected changes within individual grid cells to assess spatial variation (see below).

For individual model grid cells, we assessed response-specific scaled sensitivities as described above and then used these to generate a response index across space. This index is designed to maintain both the direction and scale of sensitivities, recognizing that some conditions evoke larger responses than others, and that different responses (e.g., growth rate and survival) with opposing signs do not necessarily combine additively to zero. For every grid cell, we aggregated species' scaled sensitivities after meta-analysis (see above) filtering to species with depth distributions included in the focal grid cell. This resulted in a distribution of weighted mean scaled sensitivities for every grid cell that ranged from negative (declines in rates) to positive (increases in rates). We defined separate indices of increases and decreases to avoid averaging-away divergent responses, as the sum of (i) increasing or (ii) decreasing responses to projected change, divided by the number of response types and species (i.e., observations), for

every grid cell. To assess each taxon's contribution to the index within each grid cell, we calculated a similar index for each taxon within each grid cell (i.e. the sum of increasing or decreasing responses across response types) to assess each taxon's contribution to the index within each grid cell. We focus on individual physiological responses to each condition and not the integrated response of an organism to multiple interacting effects of changing climate conditions, given that interactions can be synergistic or antagonistic depending on species sensitivities and ecological processes.

### 2.6 | Metabolic Index of combined temperature and oxygen sensitivities

We extended our analysis beyond the laboratory context by evaluating the combined effects of two key stressors on potential species distributions in the natural environment. Respiratory oxygen consumption is fundamentally temperature-dependent (Gillooly et al., 2001). For most species, the supply of $O_2$ (e.g., via gills) increases more slowly with temperature than does metabolic $O_2$ demand (Deutsch et al., 2021), with the result that species generally become more sensitive to low $O_2$ conditions at higher temperatures. Thus, the synergistic effects of temperature and $O_2$ in shaping physiological hypoxia sensitivity can impose more limiting constraints on species responses to environmental change than when responses to either variable are considered independently. Support for this mechanism comes from prior studies of a range of species (Clarke et al., 2021; Deutsch et al., 2021; Duncan et al., 2020; Howard, Penn, et al., 2020; McBryan et al., 2013; Penn et al., 2018; Vaquer-Sunyer & Duarte, 2011).

As an example of how this multistressor response can be evaluated, we apply the Metabolic Index ($\Phi$; Deutsch et al., 2015) framework for integrating the sensitivity of metabolism to the combined effects of $O_2$ and temperature on metabolism. This approach provides a complementary (but not strictly comparable) means of estimating species vulnerability to changing conditions. Because this framework is theoretically and experimentally grounded across diverse marine species, we use it as a stand-in for plausible responses for species without contextualizing laboratory experiments.

Specifically, $\Phi$ is the temperature-dependent ratio of organismal $O_2$ supply to demand. Physiological parameters related to the Metabolic Index and temperature-dependent hypoxia tolerance have been measured in the laboratory for dozens of species (Deutsch et al., 2021; Penn et al., 2018). Metabolic theory predicts that these organismal constraints ultimately limit population-scale processes (Van Der Meer, 2006), with an additional energetic factor, here indicated as $\Phi_{crit}$, required for critical activities like growth and reproduction above the basal metabolic demands measured experimentally. This factor is roughly 1.5–7 times greater than resting metabolism, in both marine and terrestrial animals (Deutsch et al., 2021; Peterson et al., 1990). When $\Phi/\Phi_{crit} < 1$, the environment no longer has the aerobic capacity to support the organism's regular energetic requirements. The biogeographic distributions of a number of species are closely aligned with a threshold of $\Phi/\Phi_{crit} = 1$ in depth, space, and time (Deutsch et al., 2015, 2021; Howard, Penn, et al., 2020), suggesting that this may be a useful metric for assessing climate sensitivities.

We projected changes in $\Phi/\Phi_{crit}$ between the present and future periods for northern anchovy (*Engraulis mordax*) and Alaska pink shrimp (*Pandalus eous*). Metabolic Index traits for anchovy are taken from Howard, Penn, et al. (2020). Shrimp physiological traits are assumed to be similar to those measured for the Atlantic pink shrimp (*Pandalus borealis*; Penn et al., 2018); Alaska and Atlantic pink shrimp were recently determined to be separate species (Squires, 1992) but are closely related and live in similar hydrographic conditions in each ocean basin. Observations of species presence are taken from the Ocean Biodiversity Information System (OBIS, 2019) and National Oceanic and Atmospheric Administration trawl survey data (NOAA, 2019). We used the 12 km resolution model, which encompasses the southern range limit of both species, to project hundred-year changes (2071–2100 – 1971–2000, as in Howard, Frenzel, et al., 2020) near the mean observed depths for each species.

To map habitat availability changes, we additionally delineate offshore range boundaries using species distribution models (SDMs) based on present correlations between species observations and environmental variables (see Supplementary Information); SDM offshore habitat extent is particularly sensitive to primary productivity. We did not attempt to extend the SDM approach into prediction of future habitat because these relationships are not robust under changing environmental conditions (Muhling et al., 2020), and the projected ensemble mean productivity changes cannot be distinguished from zero (Howard, Frenzel, et al., 2020).

## 3 | RESULTS

Based on the highest fossil fuel emission trajectory (RCP 8.5), by 2100, the California Current System will likely experience large changes in climate stressors such as temperature, oxygen, and $pCO_2$. Global models and downscaled simulations agree on the direction and approximate magnitude of change (Howard, Frenzel, et al., 2020) except for the ocean acidification variables whose magnitudes were modified in the downscaled projections (Siedlecki et al., 2021). Projected changes are generally similar between the two downscalings across the continental shelf (Figure 1 and Table S2), although surface $CO_2$ changes are greater in the 12 km than 1.5 km model projections (Table S2, Figure S5).

Climate-driven environmental changes are projected to be greatest in the northern-CCME (Figure 1; Siedlecki et al., 2021). The northern-CCME differs from the rest of the CCME in several ways, but importantly the region experiences a more substantial downwelling season that is anticipated to persist into the future. Oxygen removal by respiratory consumption of organic material produced over the summer is typically relieved by the fall transition and winter mixing on the shelf (Siedlecki et al., 2015), and this pattern continues into the future (Siedlecki et al., 2021). The projections indicate that the duration of very low oxygen persistence in the summer months will increase in the future projections. This seasonal pattern is also

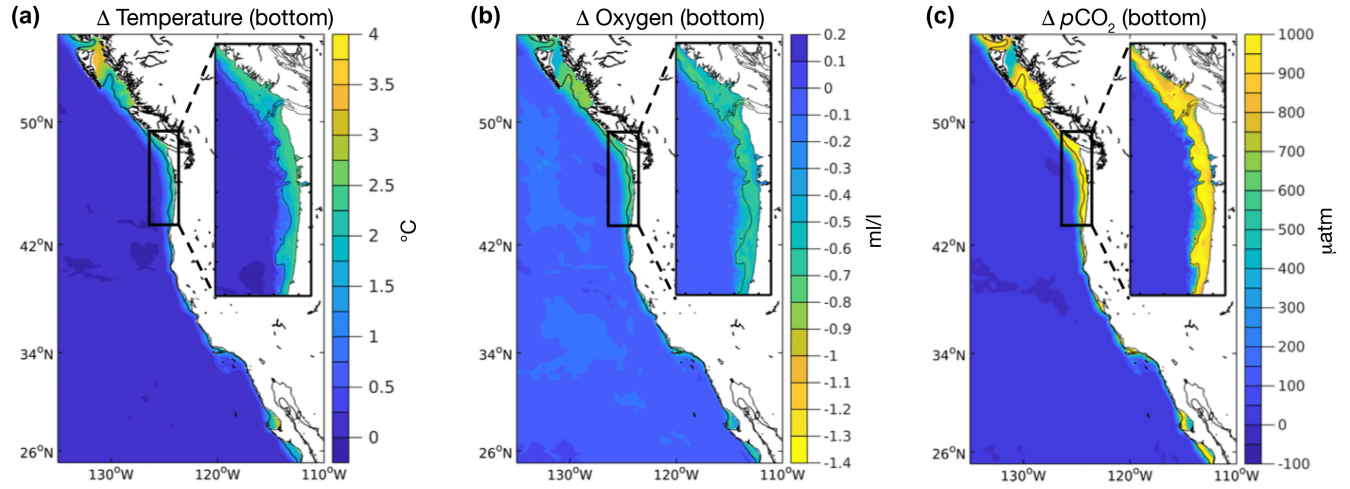


FIGURE 1 Downscaled physical model outputs for the Pacific coast of North America from British Columbia to Baja California. Each panel shows results for the large California Current Marine Ecosystem (12 km resolution model) and the smaller Cascadia region (inset; 1.5 km resolution model). Colors indicate differences between year 2100 and the base/modern conditions, in the bottom (benthic) zone of each model, for (a) temperature (deg C), (b) $O_2$ (ml/L), and (c) $pCO_2$ (µatm). For model results in the surface and 200 m zone and for other environmental variables, see Siedlecki et al. (2021). Reproduced from Siedlecki et al. (2021).

characteristic of simulated carbon variables—the most severe conditions develop over the upwelling season and are relieved in the downwelling season in the present ocean, but because of the projected increases in $pCO_2$ suboptimal carbonate chemistry conditions persist for the majority of the year in the future projections.

## 3.1 | Physiological sensitivities

Our synthesis of laboratory studies revealed a range of biological sensitivities to changes in oxygen, temperature, $pCO_2$, and pH when scaled to changes expected over the next century in the CCME (Figure 2a). Every species examined showed both increases and decreases in scaled sensitivities to projected change, differing across response types (Figure 2a). Sensitivities to changes in $pCO_2$ and pH were greater in magnitude in both positive and negative directions than were sensitivities to the other environmental variables examined (Figure 2a, blue points >50% change). Sensitivities to increasing temperature were also high (upward of 30% change), with notably more increases than decreases in biological rates in most species (i.e., rates are primarily positive in Figure 2a), except in canopy-forming kelps. Although lowest in magnitude, biological rates generally declined with projected changes in $pO_2$ across species; although we note that our linear regression across a nonlinear feeding and metabolic rate responses to $pO_2$ in Dungeness crab and sablefish, respectively, may have underestimated the sensitivity of these groups (see linear fits in Figure S3).

In the meta-analyzed results, an approximately even spread of increases and decreases in biological rates were associated with projected environmental change across species and response types (Figure 3a), and most species exhibited both increases and decreases in biological rates across response types (Figures 3b). Notably, most survival-related responses decreased, while responses in physiological rates (growth rate, metabolic rate, consumption rate, and movement) increased (Figure 3c). For example, in five species (canopy-forming kelps, razor clams, red urchins, Dungeness crab, and copper & quillback rockfish), declines in survival rates were associated with changes in projected environmental conditions, despite four of these species showing increases in physiological rates (Figure 3b). One group—the copper & quillback rockfish—showed only declining biological rates to projected changes, but studies of temperature-related responses were lacking for this group. The ochre star, by contrast, exhibited only positive physiological responses to projected changes, with no signs of decline in survivorship (Figure 3b). Although canopy-forming kelps exhibited some positive responses in growth and survival rates associated with expected changes in carbonate chemistry in individual studies (Figure 2a), these were mostly balanced by negative responses to temperature in the meta-analysis (Figure 3b). Pink salmon and sablefish showed moderate responses to projected changes, although sablefish showed a negative response to oxygen that could interact with increasing metabolic demand associated with rising temperature (Figure 3b).

The Metabolic Index values for shrimp and anchovy decline in response to concurrent oxygen loss and warming (Figure 2b). Under present hydrographic conditions, aerobic habitat limitation ($\Phi/\Phi_{crit} < 1$) closely aligned with the time–mean depth distributions and southern range limits of each species, implying that temperature-dependent hypoxia may impose an important ecophysiological constraint. Although derived using a different analytical approach, this result is consistent with both the negative sensitivity to declining $O_2$ and increasing metabolism and consumption rates with increasing temperature found in laboratory studies of other species (Figure 2a).

## 3.2 | Sensitivity variation across space

As in the whole-domain results described above, the scaled sensitivities among species and response types within each grid cell ranged

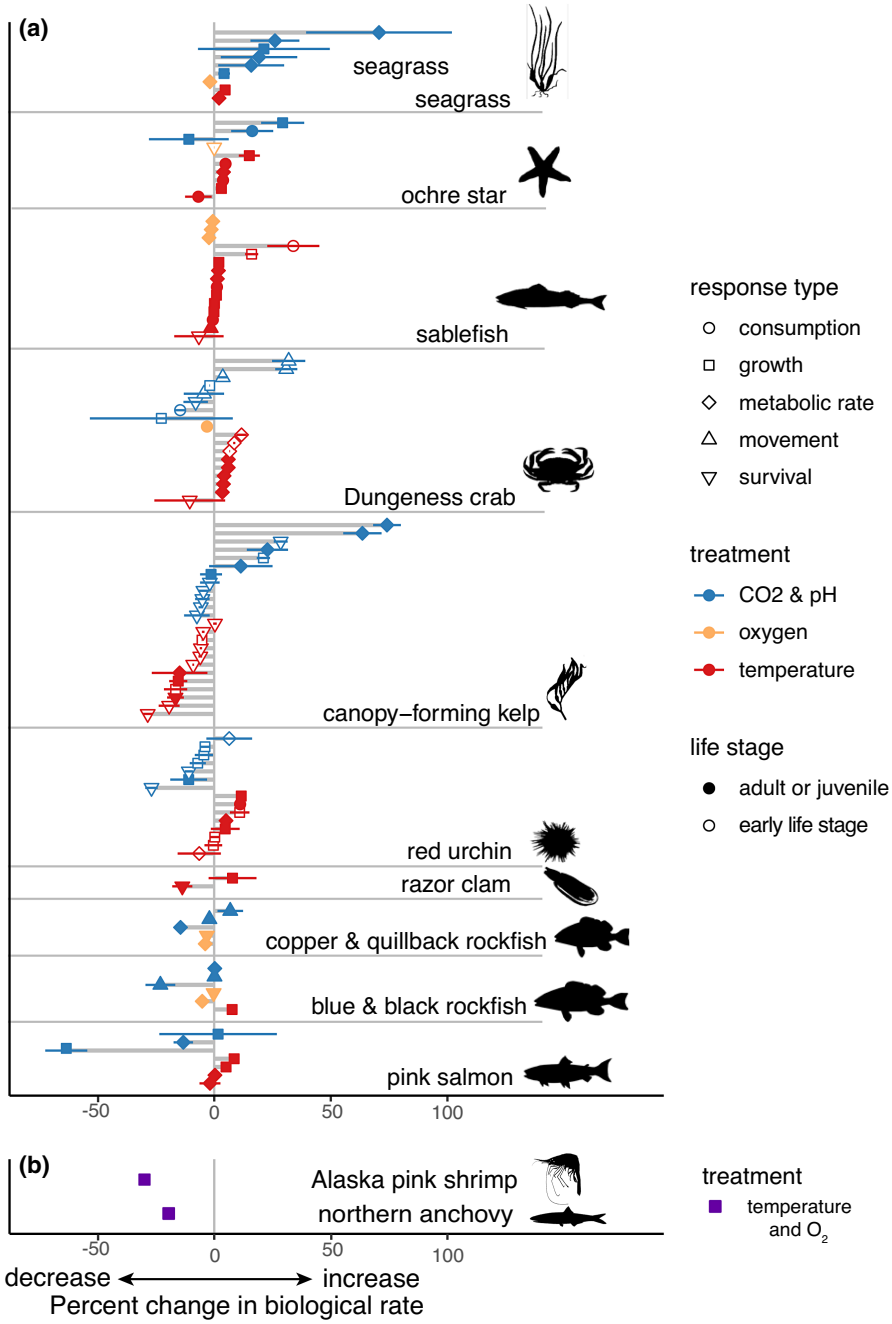


**FIGURE 2** Sensitivities to anticipated environmental change. (a) Points and horizontal lines indicate mean and 95% CI of scaled sensitivities, that is, the percent change in biological response based on fitted slopes of responses to treatment variables within study, multiplied by mean change in each treatment variable projected within the depth range of the taxon and life-history stage across the model domain (results shown for Cascadia 1.5 km model). Thus, sensitivities are shown according to the mean anticipated changes in each variable, to contextualize the sensitivity within the exposure projected, allowing comparison across variables that change at different magnitudes. Each point and error bar represents a single experiment, symbols represent specific response types, treatment variables, and life stages. Lines connecting points are provided to visually connect responses within species. Studies reporting sensitivities to changes in salinity were not sufficient to draw conclusions, so we excluded salinity from subsequent analyses (see Figure S6). (b) Sensitivities to combined temperature and oxygen changes based on Metabolic Index approach are provided for visual comparison. Silhouettes are original art generated in Adobe Photoshop by J. Sunday.

from positive to negative (Figure 4a–c), with some spatial variation. When we combined responses within model grid cells into separate positive and negative response indices (colored bars in Figure 4a–c, see Figure S7 for species identity), these were relatively equal in magnitude across most of the model domain (Figure 4d, maroon and violet cells labeled b and c). However, the positive response index was greater than the negative response index in the innermost shallow section of the shelf (Figure 4d, purple cells labeled a, *details of example cell shown in* Figure 4a), and in some regions of the mid-shelf (bluish cells; see also Figure S8 for positive and negative indices separated, and Figures S9–S10 for individual species responses). At the edge of the shelf (pink cells), negative response indices were greater than positive indices. Overall, the magnitudes of response indices declined from the inner to the outer shelf in the Cascadia region (Figure 4d,e), and from north to south in the CCME (Figure 4e; Figure S8). Spatial heterogeneity in the north–south direction was probably due to patterns in projected environmental change (as seen in Figure 1), while heterogeneity across the shelf in the east–west direction appeared to be due primarily to differences in depth ranges occupied by species across the model domain. For example, the shallow-ranging kelps, ochre stars, razor clams, red urchins, and seagrass contributed to higher response indices (more extreme positive and negative sensitivities) close to shore, and the especially high positive response in metabolic rates of kelp to increased $CO_2$ led to high positive index values in shallow water, while the inclusion of less-sensitive deep-water sablefish contributed to lower response

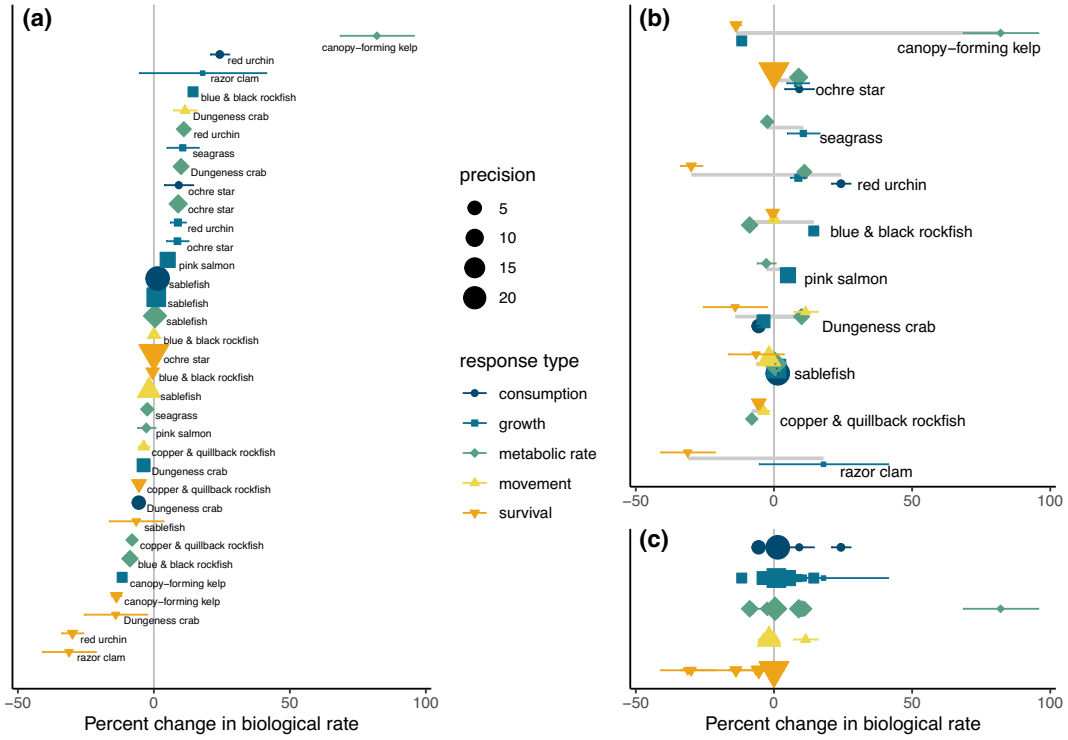


FIGURE 3 Weighted mean responses within species and response types from meta-analyses, displayed three ways. Points represent aggregated responses to all four environmental variables across the relevant layers for each taxon in the model domain, separated by response type. Means were weighted by precision of estimates from each individual study. Colored horizontal bars indicate 95% CI of each sensitivity based on meta-analysis results, and the size of each point indicates precision (1/SE of weighted mean), with larger points indicating higher precision. In (a), results are shown in order of mean response, regardless of response type and taxon; in (b), responses are organized by taxon, with gray horizontal bar indicating the span of mean responses within each taxon, and in (c), responses are organized by response type.

indices in deeper regions of the shelf (see Figures S9–S10). Within species, there was little spatial heterogeneity in index magnitude (Figures S9 and S10), which corresponds to the pattern of environmental change projected across the shelf in the Cascadia (1.5 km) and CCME (12 km) resolution models.

The Metabolic Index analysis suggests loss of aerobic habitat across the range of northern anchovy and Alaska pink shrimp in response to projected changes in temperature and $O_2$ concentrations (Figure 5). We find that both species would lose aerobically suitable habitat along their southern range limits, which could shift ranges northwards. Alaska pink shrimp were inferred to have a relatively low hypoxia tolerance and a high metabolic rate increase with temperature compared to most species (Deutsch et al., 2021). Consequently, aerobically suitable pelagic habitat for these shrimp moves offshore, leaving most of the shelf unsuitable except in the northern shelf region (Figure 5a, region left of the yellow line). Moreover, declining $O_2$ in seasonally upwelled waters will likely limit benthic habitat favored by egg-brooding female shrimp (Bergström, 2000). Northern anchovy are expected to be more hypoxia tolerant and less temperature sensitive than the shrimp; thus, aerobic habitat loss is predicted to be less severe for anchovy. However, anchovy will still likely experience increasing alongshore seasonal habitat compression across their latitudinal range (Howard, Penn, et al., 2020; Figure 5b, region north of the yellow line).

## 4 | DISCUSSION

Our findings reveal that by 2100, environmental changes projected to occur in the California Current Marine Ecosystem (CCME) will be sufficiently large to elicit changes in biological rates among a suite of economically and culturally important species. Among these, by 2100, many biological rates are expected to exceed present-day rates by more than 25% (scale in Figures 2 and 3), from which we can anticipate effects on the ecosystem (see Implications section, below). We find that individual biological responses will be more severe in the northern region of the CCME, reflecting greater relative environmental change, compared with the southern region, and greater along the inner shelf, reflecting a larger proportion of sensitive species at shallower depths, compared to the outer shelf regions. We also find projected loss of aerobic habitat in two species for which we could combine temperature and oxygen sensitivities, likely causing an aerobically driven northward retreat of their southern range edges. Although based on a thorough literature search of experimental data, our work highlights data gaps for species of high ecological and economic concern that could be readily filled with targeted experiments.

Considering multiple environmental variables (temperature, $pCO_2$, $O_2$) simultaneously allowed us to directly compare organismal sensitivities to projected changes in each of these three variables.

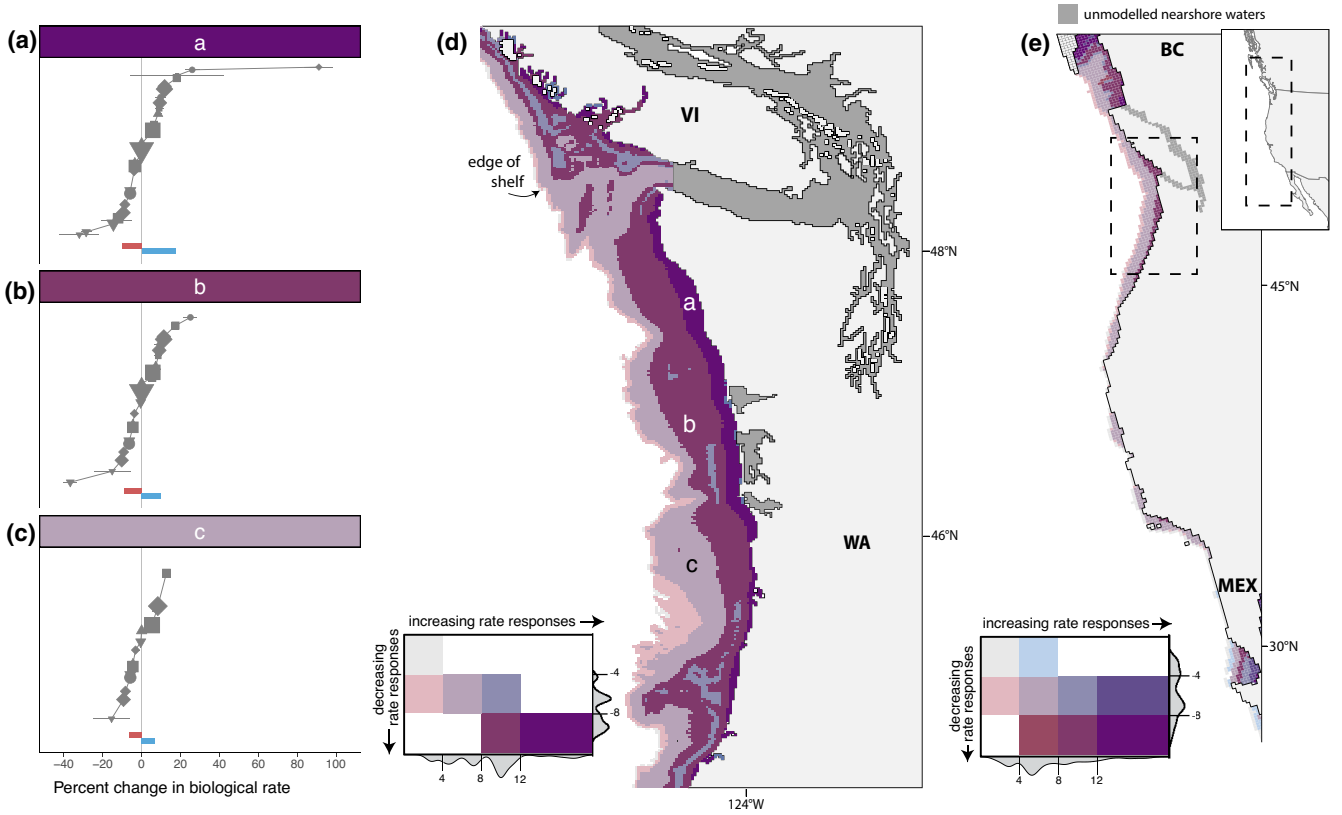


FIGURE 4 Response indices across locations along the Pacific coast of North America for the Cascadia and larger California Current Marine Ecosystem. (a–c) Scaled sensitivities of species and response types for species with depth distributions included in the three illustrative grid cells of the Cascadia 1.5 km model domain, locations indicated in panel (d). Horizontal bars indicate the combined mean increasing and decreasing responses, with values matching x and y grid in panel (d). (d–e) Positive and negative response indices within (d) the Cascadia domain (1.5 km resolution model), results for the outer shelf of Vancouver Island (VI) and Washington state (WA); and (e) the CCME domain (12 km resolution model), results for the outer shelf from British Columbia, Canada (BC) to Baja California, Mexico (MEX). Model domains do not include the inner seas (dark gray areas) or locations deeper than 500 m (indicated as the *edge of shelf*). For each grid cell in the model domains, the weighted mean of biotic responses to projected environmental changes for each species and response type (e.g., gray points in a–c) were grouped as increasing and decreasing responses, and each group summed and standardized by number of responses investigated (this index is represented as horizontal bars in a-c). Colors in d–e indicate the scale of the index, showing where mean increasing and decreasing responses to projected environmental change are relatively equal (gray, violet, and maroon cells; b and c), where increases outweigh decreases (purple cells; b), and where decreases outweigh increases (pink). The magnitude of effects generally declines from the coast to the outer shelf. Results are constrained to show the shelf and slope regions <500 m in depth, containing the depth distribution of most species. Density distributions around the color legends indicate the relative frequency of the index values in each model domain, and values indicate the threshold index values used for color display.

Overall, sensitivities to carbonate system changes were more variable across species than were sensitivities to other stressors, causing the largest decreases in individual biological rates in some species and the largest increases in others. This species-level variability is consistent with global patterns of high interspecific variability in ocean acidification sensitivities, even among taxonomically similar species (Busch & McElhany, 2016; Kroeker et al., 2013). By contrast, almost all species considered showed intermediate increases in biological rates with increased temperature. This is consistent with the expectation that temperate–latitude ectotherms tend to experience mean annual temperatures in the *rising* portion of their thermal performance curves (Deutsch et al., 2008), and hence, metabolically constrained biological rates are expected to increase with rising temperature (Gillooly et al., 2001). One exception here were the canopy-forming kelps, in which biological rates mostly declined with temperature responses, in contrast to (and potentially offsetting) the increases in physiological rates with increased $pCO_2$. In direct assays, oxygen sensitivity was moderately negative or neutral for the six species investigated. Yet for those species in which interactive oxygen and temperature sensitivities were considered together via the Metabolic Index, responses were strong and negative, highlighting the importance of the interaction between increasing temperature (and thus oxygen demand) with decreased oxygen supply.

The direction of change in biological rates varied among response types: Rates of survival almost always declined, while changes in physiological rates (growth, consumption, movement, and metabolic rate) more often increased. This finding indicates that, not surprisingly, the choice of response types used in experiments and the way in which they are combined is critical to conclusions about climate sensitivity. Furthermore, interpretation of

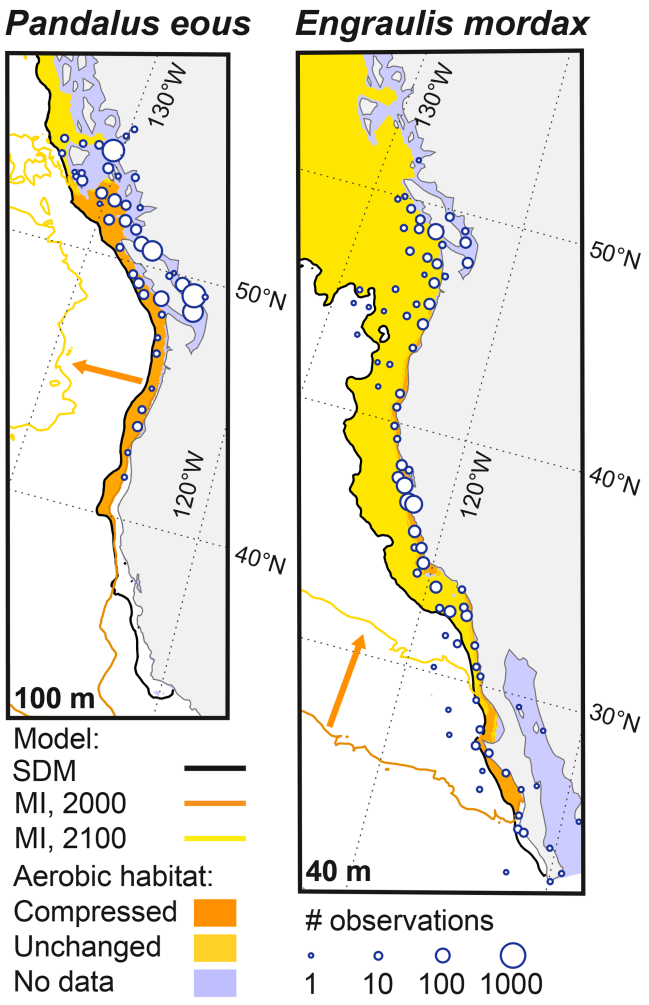


FIGURE 5 Predicted annual mean habitat limits at the median observed depths of Alaska pink shrimp (*Pandalus eous*, 100 m) and northern anchovy (*Engraulis mordax*, 40 m), using 12 km regional model outputs. Land is shown in gray, and predicted distributions are shown in yellow and orange areas, based on both the species distribution model (SDM) and the Metabolic Index (MI). Blue circles: Number of observations from all depths and years (1° binned). Black line: Edge of SDM (<50% probability offshore). Orange (1994–2007) and yellow (2100) lines: Temperature-dependent hypoxia threshold ($\Phi/\Phi_{crit}>1$ from the MI), with aerobic habitat primarily offshore (west) of line for Alaska pink shrimp and north of line for northern anchovy. Orange arrows: Spatial direction of the temporal shift in the MI threshold.

increasing physiological rates at the organism or population level is not simple: increasing physiological rates are not always beneficial to an organism, and can have detrimental effects when resources (e.g., food or oxygen) do not increase to meet demand (see below). The differing directions of rate changes among response types make it difficult to ascertain an overall species-level *climate sensitivity* via data synthesis. Our assumption of additive effects within response types and taxa provided a first approximation of overall sensitivity. We present this approximation with caution and refer often to the individual-study level data in our interpretations, because we expect non-additive effects between stressors (e.g., temperature can affect the growth rate sensitivity to $CO_2$), and nonadditive effects among life-history stage responses (mortality of a larva is not equal to mortality of a reproductive adult). Similarly, aggregating individual species and stressor-level data within grid cells allowed spatial patterns to be summarized, but this metric should also be interpreted with caution, as different responses across response types are not necessarily additive.

Interpreting the effects of physiological rate changes at higher (e.g., population) levels is similarly not straightforward. Higher physiological rates can represent greater intrinsic population growth potential, but can also represent greater resource demand. If energetic resource supply rates are limiting and do not increase to match demand, greater per-capita resource demand (e.g., higher metabolic rate) can cause declines in population growth rates or population size at carrying capacity (Bernhardt et al., 2018; Carozza et al., 2019; Gillooly et al., 2007). Although we could not do so using all species in our meta-analysis, we directly explored this mechanism with regard to oxygen limitation in our Metabolic Index approach by asking how increased metabolic demand with warming changes the minimum oxygen requirement for survival; we find that within the CCME, increased biological rates can be detrimental where oxygen supply is not simultaneously increased to meet demand.

Our Metabolic Index approach thus allowed multiple climate variables to be combined through a hypothesized mechanistic interaction. Both species examined—anchovy and pink shrimp—were projected to lose aerobic habitat at the warm edge of their ranges because temperature-driven increases in metabolic rates cannot be supported by the available oxygen supply. This is consistent with the developing understanding that temperature-dependent hypoxia presents a pervasive habitat barrier for diverse marine species (Deutsch et al., 2021). The timing and duration of aerobic stress will depend on the particular habitat and traits of species, including their relative mobility, which could allow rapid shoaling and avoidance of low $O_2$ areas. By contrast, in our meta-analysis of organismal responses, there were insufficient data on oxygen limits, nor mechanistic models allowing other combinations of climate responses, to combine them in this way. Clearly, frameworks for mechanistically combining stressors will be pivotal for projecting biological response to environmental change.

Several complexities will need to be overcome to translate the observed physiological responses presented here to projections of population or ecosystem change. First, we have modeled linear responses of biological rates to projected environmental change in mean conditions, but nonlinearities in responses (e.g., thermal performance curves) combined with variability in environmental conditions (e.g., heatwaves, low oxygen events, and other extremes) can lead to counterintuitive responses. For example, the addition of temporal variability in the temperature dimension causes organisms to experience population declines at mean temperatures that are seemingly benign due to nonlinear declines beyond the thermal optimum (Bernhardt et al., 2018; Martin & Huey, 2008; Vasseur et al., 2014). The response to oxygen in Dungeness crab and sablefish, for example, was nonlinear and steeper at lower $O_2$ values

(Figure S3), leading to underestimates of oxygen sensitivity in these species in our analysis. Similarly, some declines in biological rates at high temperatures lead to underestimates of rate declines, depending on the temperatures experienced (Figure S2); future analyses that capture value-specific responses rather than an overall sensitivity are warranted. Second, responses at one life-history stage may be nonadditively offset by stronger (positive or negative) responses at another stage through demographic compensation (Doak & Morris, 2010; Le Quesne & Pinnegar, 2012). Here, we combined responses among life-history phases additively, but the sensitivity of juvenile phases (constituting much of the data from Dungeness crab, red urchins, and kelp) may have smaller demographic effects due to lower reproductive potential of early life stages compared to adults (Kindsvater et al., 2016), or can be critical transition stages causing demographic bottlenecks (Dahlke et al., 2020). Third, interactions between species are expected to drive changes in community structure that could be at odds with species-specific predictions (Doney et al., 2020; Gilbert et al., 2014; Gilman et al., 2010). Results from an ecosystem modeling framework exemplify these last two points with responses to $pCO_2$ among CCME species, as reported by Marshall et al. (2017). These authors used an end-to-end ecosystem model forced by climate projections of seawater pH in the CCME, informed by a meta-analysis of the pH sensitivities (Busch & McElhany, 2016). In their modeling, the direct negative effects of ocean acidification on Dungeness crab larvae failed to manifest at the population level due to demographic compensation of adults, whereas reductions in their prey populations—caused by negative responses to ocean acidification in other species—resulted in projected declines in Dungeness crab populations. Our results are consistent with those of Marshall et al. (2017) in finding clear negative sensitivities to $pCO_2$ among some epibenthic invertebrates and groundfish (Dungeness crabs, red urchins, and rockfish) —although in our study these are derived only from direct responses (without a trophic interaction). Our work generally differs by focussing on taxon-specific data, summarizing response rates as slopes (and thus accounting for different treatment levels among studies), and providing the additional context of responses to $O_2$ and temperature. Although we do not place our results within an ecosystem model, we consider some community-scale implications via species interactions (see Ecological Implications, below).

## 4.1 | Data gaps

Our synthesis identified data gaps of considerably high priority. First, it was surprising how few response types and corresponding environmental variables have been reported for the species we examined, given their socio-economic importance. The coverage across species, treatments (temperature, $O_2$, $pCO_2$, or pH), and response types was low (median coverage within species = 37%, max coverage = 47%) and this issue persisted even after reducing the species set due to data scarcity, combining some species into groups (canopy-forming kelps, rockfish species pairs), and excluding salinity due to insufficient data. Experimentally derived responses to low $O_2$ were especially sparse in the literature, despite the expected declines in $O_2$ in this region and the importance of direct $O_2$ limitation and $O_2$-limited thermal tolerance among regional species. Moreover, most studies of survival were conducted on larval stages but not on adults, leaving open questions about variation in response strength across life stages, and resulting demographic responses. Furthermore, it was not possible to incorporate empirically derived responses to multiple drivers as would be required to estimate their interactive effects, simply because the experimental data were mostly lacking. Physiological experiments focused on responses to global change seem often have used "model" species rather than those of cultural and economic concern, often focus on single life-history phases, and rarely consider all three key environmental stressors or their interactions. It is within reach to fill these gaps with efficient, complexity-focussed experimental designs (e.g., factorial, collapsed, or reduced designs, reviewed in Boyd et al., 2018) that consider multiple life-history stages.

While our dataset describing physiological sensitivities could have been augmented by adding correlational responses to environmental change or including data generated from closely related species, we chose to constrain our input data to controlled experiments on the particular species of interest. Doing so increases our confidence that the mechanisms underpinning the observed sensitivities are actually related to the specified variables. Although the Metabolic Index approach requires even more information for each species—namely, an estimate of threshold values for oxygen limitation at multiple temperatures—the value of the data for projecting the interactive impacts of multiple stressors warrants the added experimentation required. Given our observation of differing overall trends between survival and other biological rates, we emphasize as a priority the need to assess responses that are most likely to influence demographic processes (e.g., through changes in survival and reproduction) for species of cultural and economic concern in the CCME.

## 4.2 | Scaling results across space and time

Our approach combines high-resolution climate projections with experimentally derived biological responses to estimate vulnerability to changing ocean conditions. However, in most cases, experimental organisms were collected from a single site within the CCME, thereby constraining the available genetic and physiological potential in unknown ways and leading to the possibility that unobserved phenotypic variation in response norms could lead to different responses across the species' range. Similarly, the conditions in laboratory assays (e.g., food supply, oxygen availability, levels of other stressors, age and condition of experimental subjects) can influence results, and it is not possible to evaluate responses to changes in these covariates without factorial experiments (Doney et al., 2020). Moreover, using responses measured in the past to understand sensitivity in the future does not allow the possibility of adaptation and acclimation within that time frame. However, we note that over seasonal to interdecadal

periods, biogeographical retreat in response to adverse conditions appears to be more common than physiological change across a range of water-breathing ectotherms (e.g., Deutsch et al., 2015; Fredston-Hermann et al., 2020; Hastings et al., 2020; Morley et al., 2018; Pinsky et al., 2013). Taken together, the experimental data provide a coarse but data-driven lens through which to understand the relative sensitivity of species of concern in the CCME.

### 4.3 | Ecological implications

Our results suggest that substantial levels of change can be expected within this century for every taxon included in our analysis in every grid cell of the CCME inner shelf region. Moreover, such changes are highly unlikely to be restricted to the suite of species examined here, and can reasonably be expected to occur across species yet unstudied. Such widespread change will, over time, cause substantial changes in ecosystem structure and function. Local or regional loss of canopy-forming kelps caused by declining rates of survival and growth can affect local biodiversity through loss of structural habitat (Arkema et al. 2009), and potentially alter other ecosystem services provided by kelp (Norderhaug et al., 2020); although kelps had high positive responses in metabolic rate, it is unclear how these will interact with declines in survival and growth. Increased growth and consumption rates in two invertebrate species with strong interactions, red urchins (reviewed in Rogers-Bennett, 2007) and ochre stars (Paine, 1966), could have large knock-on effects on nearshore food webs if left unchecked, as observed in the 2014 sea star wasting disease epidemic, in which ochre stars and their predation rates declined (Menge et al., 2016). Controlled experiments on survival responses to climate change of both species are currently only available for their larval stages, with evidence that red urchin larvae will have decreased survival; clearly further study into demographic effects and adult survival is warranted for these taxa. Reduction or loss of species of cultural and commercial value caused by reduced survival among Dungeness crab, razor clams, sablefish, and copper and quillback rockfish (Figure 3b), and loss of aerobic habitat for anchovy and pink shrimp (Figure 5), all can be expected by the end of this century with expected impacts on human livelihoods. These outcomes could be mitigated or exacerbated by changes in other interacting species. For example, changes in food or nutrient resource supply, arrival of non-native or range-expanding species (Pinsky et al., 2020), and new disease outbreaks associated with warming waters (Burge & Hershberger, 2020), could each result in changes beyond the direct sensitivities synthesized here. The socio-economic consequences of these changes are likely to be substantial and will be spread inequitably across economic sectors and human communities (e.g., Jardine et al., 2020), contributing to disparities in the potential for adaptations that promote human well-being.

Actions to maintain and expand ocean monitoring networks, further develop predictive models, integrate scientific information into the policy and decision-making domains, create and implement adaptation strategies, and promote public understanding could help to alleviate some of the anticipated harm to human communities. Even so, the scope of change over just a few generations is likely to be large, and policy interventions, while necessary, may be insufficient to fully reduce harm. Ultimately, sharp reduction in fossil fuel-derived $CO_2$ emissions is the single strategy to offer long-term benefits across all domains and is paramount to achieving success through any other intervention.

## ACKNOWLEDGMENTS

This work was supported by funding from the Schwab Charitable Fund made possible by the generosity of Wendy and Eric Schmidt, with additional support from the Washington Ocean Acidification Center. Further support was provided to group members as follows: J.S. was partially supported by the Natural Science and Engineering Research Council of Canada, the Alfred P. Sloan Foundation, and William Dawson Scholar fund, J.N. was partially supported by NOAA award NA16NOS0120019, C.D. was supported by the National Science Foundation (OCE-1635632, OCE-1847687, OCE-1419323, OCE-1737282), the National Oceanic and Atmospheric Administration Competitive Research Program (NA15NOS4780186, NA15NOS4780192, NA18NOS4780167), the California Ocean Protection Council, under Grant Agreement #C0303000 (R/OPCOAH-1) through the California Sea Grant College Program, and the Gordon and Betty Moore Foundation (GBMF3775), D.P. was partially funded by the Joint Institute for the Study of the Atmosphere and Ocean (JISAO) under NOAA Cooperative Agreement NA15OAR4320063; the views expressed herein do not necessarily reflect the views of any of those organizations. This is JISAO contribution number 2021-1159, PMEL contribution number 5120, and Eco-FOCI-1016. We gratefully acknowledge the expert advice and support of K.A. Smith Mislan in implementing the species distribution models, and the outstanding technical assistance of H. Frenzel in producing the climate projections and 12 km regional model fields.

## CONFLICT OF INTEREST

The authors have no conflict of interest to declare.

## DATA AVAILABILITY STATEMENT

The data and code that support the findings of this study are openly available in the Github repository, https://github.com/jennsunday/downscaled_sensitivities_CCME. Experimental responses dataset further archived on FigShare, https://figshare.com/articles/dataset/compiled_climate_response_data_CCME/20277705

## ORCID

*Jennifer M. Sunday* https://orcid.org/0000-0001-9372-040X
*Evan Howard* https://orcid.org/0000-0002-1993-0692
*Samantha Siedlecki* https://orcid.org/0000-0002-5662-7326
*Darren J. Pilcher* https://orcid.org/0000-0002-0763-3236
*Curtis Deutsch* https://orcid.org/0000-0003-3923-0797
*Parker MacCready* https://orcid.org/0000-0002-8070-8062
*Jan Newton* https://orcid.org/0000-0002-2551-1830
*Terrie Klinger* https://orcid.org/0000-0003-2430-0246

## REFERENCES


Arkema, K. K., Reed, D. C., & Schroeter, S. C. (2009). Direct and indirect effects of giant kelp determine benthic community structure and dynamics. *Ecology*, *90*(11), 3126–3137. https://doi.org/10.1890/08-1213.1

Bednaršek, N., Feely, R. A., Howes, E. L., Hunt, B. P. V., Kessouri, F., León, P., Lischka, S., Maas, A. E., McLaughlin, K., Nezlin, N. P., Sutula, M., & Weisberg, S. B. (2019). Systematic review and meta-analysis toward synthesis of thresholds of ocean acidification impacts on calcifying pteropods and interactions with warming. *Frontiers in Marine Science*, *6*(00227), 1–16. https://doi.org/10.3389/fmars.2019.00227

Bergström, B. I. (2000). The biology of Pandalus. *Advances in Marine Biology*, *38*, 55–245. https://doi.org/10.1016/s0065-2881(00)38003-8

Bernhardt, J. R., Sunday, J. M., & O'Connor, M. I. (2018). Metabolic theory and the temperature-size rule explain the temperature dependence of population carrying capacity. *The American Naturalist*, *192*(6), 687–697. https://doi.org/10.1086/700114

Boyd, P. W., Collins, S., Dupont, S., Fabricius, K., Gattuso, J. P., Havenhand, J., Hutchins, D. A., Riebesell, U., Rintoul, M. S., Vichi, M., Biswas, H., Ciotti, A., Gao, K., Gehlen, M., Hurd, C. L., Kurihara, H., McGraw, C. M., Navarro, J. M., Nilsson, G. E., … Pörtner, H. O. (2018). Experimental strategies to assess the biological ramifications of multiple drivers of global ocean change—A review. *Global Change Biology.*, *24*(6), 2239–2261. https://doi.org/10.1111/gcb.14102

Burge, C. A., & Hershberger, P. K. (2020). Climate change can drive marine diseases. In *Marine disease ecology* (pp. 83–94). Oxford University Press. https://doi.org/10.1093/oso/9780198821632.003.0005

Busch, D. S., & McElhany, P. (2016). Estimates of the direct effect of seawater pH on the survival rate of species groups in the California current ecosystem. *PLoS One*, *11*(8), e0160669. https://doi.org/10.1371/journal.pone.0160669

Carozza, D. A., Bianchi, D., & Galbraith, E. D. (2019). Metabolic impacts of climate change on marine ecosystems: Implications for fish communities and fisheries. *Global Ecology and Biogeography*, *28*(2), 158–169. https://doi.org/10.1111/geb.12832

Chan, F., Barth, J. A., Lubchenco, J., Kirincich, A., Weeks, H., Peterson, W. T., & Menge, B. A. (2008). Emergence of anoxia in the California current large marine ecosystem. *Science*, *319*(5865), 920. https://doi.org/10.1126/science.1149016

Clarke, T. M., Wabnitz, C. C. C., Striegel, S., Frölicher, T. L., Reygondeau, G., & Cheung, W. W. L. (2021). Aerobic growth index (AGI): An index to understand the impacts of ocean warming and deoxygenation on global marine fisheries resources. *Progress in Oceanography*, *195*, 102588. https://doi.org/10.1016/j.pocean.2021.102588

Connolly, T. P., Hickey, B. M., Geier, S. L., & Cochlan, W. P. (2010). Processes influencing seasonal hypoxia in the northern California current system. *Journal of Geophysical Research: Oceans*, *115*(3), C03021. https://doi.org/10.1029/2009JC005283

Crain, C. M., Kroeker, K., & Halpern, B. S. (2008). Interactive and cumulative effects of multiple human stressors in marine systems. *Ecology Letters*, *11*, 1304–1315.

Dahlke, F. T., Wohlrab, S., Butzin, M., & Pörtner, H.-O. (2020). Thermal bottlenecks in the lifecycle define climate vulnerability of fish. *Science*, *369*(6499), 65–70. https://doi.org/10.1126/science.aaz3658

Deutsch, C., Ferrel, A., Seibel, B., Pörtner, H.-O., & Huey, R. (2015). Climate change tightens a metabolic constraint on marine habitats. *Science*, *348*(6239), 1132–1135. https://doi.org/10.1126/science.aaa1605

Deutsch, C., Frenzel, H., Mcwilliams, J. C., Renault, L., Kessouri, F., Howard, E., Liang, J. H., Bianchi, D., & Yang, S. (2021). Biogeochemical variability in the California current system. *Progress in Oceanography*, *196*(102565), 1–35. https://doi.org/10.1016/j.pocean.2021.102565

Deutsch, C. A., Tewksbury, J. J., Huey, R. B., Sheldon, K. S., Ghalambor, C. K., Haak, D. C., & Martin, P. R. (2008). Impacts of climate warming on terrestrial ectotherms across latitude. *Proceedings of the National Academy of Sciences of the United States of America*, *105*(18), 6668–6672. https://doi.org/10.1073/pnas.0709472105

Doak, D. F., & Morris, W. F. (2010). Demographic compensation and tipping points in climate-induced range shifts. *Nature*, *467*(7318), 959–962. https://doi.org/10.1038/nature09439

Doney, S. C., Busch, D. S., Cooley, S. R., & Kroeker, K. J. (2020). The impacts of ocean acidification on marine ecosystems and reliant human communities. *Annual Review of Environment and Resources*, *45*, 83–112. https://doi.org/10.1146/annurev-environ-012320-083019

Duncan, M. I., James, N. C., Potts, W. M., & Bates, A. E. (2020). Different drivers, common mechanism; the distribution of a reef fish is restricted by local-scale oxygen and temperature constraints on aerobic metabolism. *Conservation Physiology*, *8*(1), 1–16. https://doi.org/10.1093/conphys/coaa090

Feely, R. A., Sabine, C. L., Hernandez-Ayon, J. M., Ianson, D., & Hales, B. (2008). Evidence for upwelling of corrosive "acidified" water onto the continental shelf. *Science*, *320*(5882), 1490–1492. https://doi.org/10.1126/science.1155676

Fredston-Hermann, A., Selden, R., Pinsky, M., Gaines, S. D., & Halpern, B. S. (2020). Cold range edges of marine fishes track climate change better than warm edges. *Global Change Biology*, *26*(5), 2908–2922. https://doi.org/10.1111/gcb.15035

Gattuso, J.-P., Magnan, A., Cheung, W. W. L., Howes, E. L., Joos, F., Allemand, D., Bopp, L., Cooley, S. R., Eakin, C. M., Kelly, R. P., Rogers, A. D., Baxter, J. M., Laffoley, D., Osborn, D., Rankovic, A., Rochette, J., Sumaila, U. R., Treyer, S., & Turley, C. (2015). Contrasting futures for ocean and society from different anthropogenic $CO_2$ emissions scenarios. *Science*, *349*(6243), 1–10. https://doi.org/10.1126/science.aac4722

Gilbert, B., Tunney, T. D., Mccann, K. S., Delong, J. P., Vasseur, D. A., Savage, V., Shurin, J. B., Dell, A. I., Barton, B. T., Harley, C. D. G., Kharouba, H. M., Kratina, P., Blanchard, J. L., Clements, C., Winder, M., Greig, H. S., & O'Connor, M. I. (2014). A bioenergetic framework for the temperature dependence of trophic interactions. *Ecology Letters*, *17*(8), 902–914. https://doi.org/10.1111/ele.12307

Gillooly, J. F., Brown, J. H., West, G. B., Savage, V. M., & Charnov, E. L. (2001). Effects of size and temperature on metabolic rate. *Science*, *293*(5538), 2248–2251. https://doi.org/10.1126/science.1061967

Gillooly, J. F., McCoy, M. W., & Allen, A. P. (2007). Effects of metabolic rate on protein evolution. *Biology Letters*, *3*(6), 655–660. https://doi.org/10.1098/rsbl.2007.0403

Gilman, S. E., Urban, M. C., Tewksbury, J., Gilchrist, G. W., & Holt, R. D. (2010). A framework for community interactions under climate change. *Trends in Ecology and Evolution*, *25*(6), 325–331. https://doi.org/10.1016/j.tree.2010.03.002

Hare, J. A., Morrison, W. E., Nelson, M. W., Stachura, M. M., Teeters, E. J., Griffis, R. B., Alexander, M. A., Scott, J. D., Alade, L., Bell, R. J., Chute, A. S., Curti, K. L., Curtis, T. H., Kircheis, D., Kocik, J. F., Lucey, S. M., McCandless, C. T., Milke, L. M., Richardson, D. E., … Griswold, C. A. (2016). A vulnerability assessment of fish and invertebrates to climate change on the northeast U.S. continental shelf. *PLoS One*, *11*(2), e0146756. https://doi.org/10.1371/journal.pone.0146756

Hastings, R. A., Rutterford, L. A., Freer, J. J., Collins, R. A., Simpson, S. D., & Genner, M. J. (2020). Climate change drives poleward increases and equatorward declines in marine species. *Current Biology*, *30*(8), 1572–1577. https://doi.org/10.1016/j.cub.2020.02.043

Henson, S. A., Beaulieu, C., Ilyina, T., John, J. G., Long, M., Séférian, R., Tjiputra, J., & Sarmiento, J. L. (2017). Rapid emergence of climate change in environmental drivers of marine ecosystems. *Nature Communications*, *8*(1), 1–9. https://doi.org/10.1038/ncomms14682

Hodgson, E. E., Kaplan, I. C., Marshall, K. N., Leonard, J., Essington, T. E., Busch, D. S., Fulton, E. A., Harvey, C. J., Hermann, A. J., & McElhany, P.

(2018). Consequences of spatially variable ocean acidification in the California current: Lower pH drives strongest declines in benthic species in southern regions while greatest economic impacts occur in northern regions. *Ecological Modelling*, *383*, 106–117. https://doi.org/10.1016/j.ecolmodel.2018.05.018

Hollowed, A. B., Holsman, K. K., Haynie, A. C., Hermann, A. J., Punt, A. E., Aydin, K., Ianelli, J. N., Kasperski, S., Cheng, W., Faig, A., Kearney, K. A., Reum, J. C. P., Spencer, P., Spies, I., Stockhausen, W., Szuwalski, C. S., Whitehouse, G. A., & Wilderbuer, T. K. (2020). Integrated modeling to evaluate climate change impacts on coupled social-ecological Systems in Alaska. *Frontiers in Marine Science*, *6*, 775. https://doi.org/10.3389/fmars.2019.00775

Howard, E. M., Frenzel, H., Kessouri, F., Renault, L., Bianchi, D., McWilliams, J. C., & Deutsch, C. (2020). Attributing causes of future climate change in the California current system with multi-model downscaling. *Global Biogeochemical Cycles*, *34*, e2020GB006646. https://doi.org/10.1029/2020GB006646

Howard, E. M., Penn, J. L., Frenzel, H., Seibel, B. A., Bianchi, D., Renault, L., Kessouri, F., Sutula, M. A., McWilliams, J. C., & Deutsch, C. (2020). Climate-driven aerobic habitat loss in the California current system. *Science Advances*, *6*(20), 1–11. https://doi.org/10.1126/sciadv.aay3188

Jardine, S. L., Fisher, M. C., Moore, S. K., & Samhouri, J. F. (2020). Inequality in the economic impacts from climate shocks in fisheries: The case of harmful algal blooms. *Ecological Economics*, *176*, 106691. https://doi.org/10.1016/j.ecolecon.2020.106691

Kindsvater, H. K., Mangel, M., Reynolds, J. D., & Dulvy, N. K. (2016). Ten principles from evolutionary ecology essential for effective marine conservation. *Ecology and Evolution*, *6*(7), 2125–2138. https://doi.org/10.1002/ece3.2012

Kroeker, K. J., Kordas, R. L., Crim, R., Hendriks, I. E., Ramajo, L., Singh, G. S., Duarte, C. M., & Gattuso, J. P. (2013). Impacts of ocean acidification on marine organisms: Quantifying sensitivities and interaction with warming. *Global Change Biology*, *19*(6), 1884–1896. https://doi.org/10.1111/gcb.12179

Le Quesne, W. J. F., & Pinnegar, J. K. (2012). The potential impacts of ocean acidification: Scaling from physiology to fisheries*. *Fish and Fisheries*, *13*(3), 333–344. https://doi.org/10.1111/j.1467-2979.2011.00423.x

Lewis, E. R., & Wallace, D. W. R. (1998). *Program developed for $CO_2$ system calculations. Rep. BNL-61827.* U.S. Dep. of Energy, Oak Ridge Natl. Lab., Carbon Dioxide Inf. Anal. Cent.

Lipsey, M., & Wilson, D. (2001). *Practical meta-analysis*. Sage. Retrieved from https://psycnet.apa.org/record/2000-16602-000

Marshall, K. N., Kaplan, I. C., Hodgson, E. E., Hermann, A., Busch, D. S., McElhany, P., Essington, T. E., Harvey, C. J., & Fulton, E. A. (2017). Risks of ocean acidification in the California current food web and fisheries: Ecosystem model projections. *Global Change Biology*, *23*(4), 1525–1539. https://doi.org/10.1111/gcb.13594

Martin, T. L., & Huey, R. B. (2008). Why "suboptimal" is optimal: Jensen's inequality and ectotherm thermal preferences. *American Naturalist*, *171*(3), 102–118. https://doi.org/10.1086/527502

McBryan, T. L., Anttila, K., Healy, T. M., & Schulte, P. M. (2013). Responses to temperature and hypoxia as interacting stressors in fish: Implications for adaptation to environmental change. *Integrative and Comparative Biology*, *53*(4), 648–659. https://doi.org/10.1093/icb/ict066

McCabe, R. M., Hickey, B. M., Kudela, R. M., Lefebvre, K. A., Adams, N. G., Bill, B. D., Gulland, F. M. D., Thomson, R. E., Cochlan, W. P., & Trainer, V. L. (2016). An unprecedented coastwide toxic algal bloom linked to anomalous ocean conditions. *Geophysical Research Letters*, *43*(19), 10366–10376. https://doi.org/10.1002/2016GL070023

Menge, B. A., Cerny-Chipman, E. B., Johnson, A., Sullivan, J., Gravem, S., & Chan, F. (2016). Sea star wasting disease in the keystone predator *Pisaster ochraceus* in Oregon: Insights into differential population impacts, recovery, predation rate, and temperature effects from long-term research. *PLoS One*, *11*(5), 1–28. https://doi.org/10.1371/journal.pone.0153994

Morley, J. W., Selden, R. L., Latour, R. J., Frölicher, T. L., Seagraves, R. J., & Pinsky, M. L. (2018). Projecting shifts in thermal habitat for 686 species on the north American continental shelf. *PLoS One*, *13*(5), 1–28. https://doi.org/10.1371/journal.pone.0196127

Muhling, B. A., Brodie, S., Smith, J. A., Tommasi, D., Gaitan, C. F., Hazen, E. L., Jacox, M. G., Auth, T. D., & Brodeur, R. D. (2020). Predictability of species distributions deteriorates under novel environmental conditions in the California current system. *Frontiers in Marine Science*, *7*, 1–22. https://doi.org/10.3389/fmars.2020.00589

National Oceanic and Atmospheric Administration Northwest Fishery Science Center. (2019). Trawling records of *Engraulis mordax* from West Coast groundfish bottom trawl surveys. NWFSC Fishery Resource Analysis and Monitoring Data Warehouse. https://www.nwfsc.noaa.gov/data/

Norderhaug, K. M., Filbee-Dexter, K., Freitas, C., Birkely, S. R., Christensen, L., Mellerud, I., Thormar, J., van Son, T., Moy, F., Vázquez Alonso, M., & Steen, H. (2020). Ecosystem-level effects of large-scale disturbance in kelp forests. *Marine Ecology Progress Series*, *656*, 163–180. https://doi.org/10.3354/meps13426

OBIS and Data Contributors. (2019). Distribution records of *Engraulis mordax* (Girard 1854), and other species, 1953–2015. OBIS data server. http://iobis.org/

Paine, R. T. (1966). Food web complexity and species diversity. *The American Naturalist*, *100*(910), 65–75.

Pecl, G. T., Araújo, M. B., Bell, J. D., Blanchard, J., Bonebrake, T. C., Chen, I.-C., Clark, T. D., Colwell, R. K., Danielsen, F., Evengård, B., Falconi, L., Ferrier, S., Frusher, S., Garcia, R. A., Griffis, R. B., Hobday, A. J., Janion-Scheepers, C., Jarzyna, M. A., Jennings, S., … Williams, S. E. (2017). Biodiversity redistribution under climate change: Impacts on ecosystems and human well-being. *Science*, *355*(6332), eaai9214. https://doi.org/10.1126/science.aai9214

Penn, J., Deutsch, C., Payne, J., & Sperline, E. (2018). Temperature-dependent hypoxia explains biogeography and severity of end-Permian marine mass extinction. *Science*, *362*(6419), eaat1327. https://doi.org/10.1126/science.aat1327

Peterson, C. C., Nagy, K. A., & Diamond, J. (1990). Sustained metabolic scope. *Proceedings of the National Academy of Sciences*, *87*(6), 2324–2328.

Pinsky, M. L., Selden, R. L., & Kitchel, Z. J. (2020). Climate-driven shifts in marine species ranges: Scaling from organisms to communities. In *Annual review of marine science*. Annual Reviews Inc. https://doi.org/10.1146/annurev-marine-010419-010916

Pinsky, M. L., Worm, B., Fogarty, M. J., Sarmiento, J. L., & Levin, S. A. (2013). Marine taxa track local climate velocities. *Science*, *341*(6151), 1239–1242. https://doi.org/10.1126/science.1239352

Pörtner, H.-O., Karl, D. M., Boyd, P. W., Cheung, W. W. L., Lluch-Cota, S. E., Nojiri, Y., Schmidt, D. N., & Zavialov, P. O. (2014). Ocean systems. In *Climate change 2014: Impacts, adaptation, and vulnerability. Part A: Global and Sectoral Aspects. Contribution of Working Group II to the Fifth Assessment Report of the Intergovernmental Panel on Climate Change* (pp. 411–484). Cambridge University Press.

Rogers-Bennett, L. (2007). The ecology of Strongylocentrotus franciscanus and Strongylocentrotus purpuratus. *Developments in Aquaculture and Fisheries Science*, *37*, 393–425.

Rohatgi, A. (2018). WebPlotDigitizer Version: 4.5. https://automeris.io/WebPlotDigitizer

Siedlecki, S. A., Banas, N. S., Davis, K. A., Giddings, S., Hickey, B. M., MacCready, P., Connolly, T., & Geier, S. (2015). Seasonal and interannual oxygen variability on the Washington and Oregon continental shelves. *Journal of Geophysical Research: Oceans*, *120*(2), 608–633. https://doi.org/10.1002/2014JC010254

Siedlecki, S. A., Pilcher, D., Howard, E. M., Deutsch, C., MacCready, P., Norton, E. L., Frenzel, H., Newton, J., Feely, R. A., Alin, S. R., & Klinger, T. (2021). Coastal processes modify projections of

some climate-driven stressors in the California current system. *Biogeosciences*, *18*, 2871–2890. https://doi.org/10.5194/bg-18-2871-2021

Spencer, P. D., Hollowed, A. B., Sigler, M. F., Hermann, A. J., & Nelson, M. W. (2019). Trait-based climate vulnerability assessments in data-rich systems: An application to eastern Bering Sea fish and invertebrate stocks. *Global Change Biology*, *25*(11), 3954–3971. https://doi.org/10.1111/gcb.14763

Squires, H. J. (1992). Recognition of Pandalus Eous Makarov, 1935, as a Pacific species not a variety of the Atlantic Pandalus Borealis Krøyer, 1838 (Decapoda, Caridea). *Crustaceana*, *63*(3), 257–262. https://doi.org/10.1163/156854092X00406

Van Der Meer, J. (2006). Metabolic theories in ecology. *Trends in Ecology and Evolution*, *21*(3), 136–140. https://doi.org/10.1016/j.tree.2005.11.004

Vaquer-Sunyer, R., & Duarte, C. M. (2011). Temperature effects on oxygen thresholds for hypoxia in marine benthic organisms. *Global Change Biology*, *17*(5), 1788–1797. https://doi.org/10.1111/j.1365-2486.2010.02343.x

Vasseur, D. A., DeLong, J. P., Gilbert, B., Greig, H. S., Harley, C. D. G., McCann, K. S., Savage, V., Tunney, T. D., & O'Connor, M. I. (2014). Increased temperature variation poses a greater risk to species than climate warming. *Proceedings of the Royal Society B: Biological Sciences*, *281*(1779), 20132612. https://doi.org/10.1098/rspb.2013.2612

## SUPPORTING INFORMATION

Additional supporting information may be found in the online version of the article at the publisher's website.

**How to cite this article:** Sunday, J. M., Howard, E., Siedlecki, S., Pilcher, D. J., Deutsch, C., MacCready, P., Newton, J., & Klinger, T. (2022). Biological sensitivities to high-resolution climate change projections in the California current marine ecosystem. *Global Change Biology*, *28*, 5726–5740. https://doi.org/10.1111/gcb.16317